Proceedings of the 2nd Biennial IEEE/RAS-EMBS International
Conference on Biomedical Robotics and Biomechatronics
Scottsdale, AZ, USA, October 19-22, 2008

Real-Time Isometric Pinch Force Prediction from sEMG

Changmok Choi, *Student Member, IEEE*, Suncheol Kwon, Wonil Park, Mihye Shin, and Jung Kim, *Member, IEEE*

***Abstract*— This paper describes a real-time isometric pinch force prediction algorithm using surface electromyogram (sEMG). The activities of seven muscles related to the movements of the thumb and index finger joints, which are observable using surface electrodes, were recorded during pinch force experiments. For the successful implementation of the real-time prediction algorithm, an off-line analysis was performed using the recorded activities. From the seven muscles, four muscles were selected for monitoring using the Fisher linear discriminant paradigm in an off-line analysis, and the recordings from these four muscles provided the most effective information for mapping sEMG to the pinch force. An ANN structure was designed to perform efficient training and to avoid both under-fitting and over-fitting problems. Finally, the pinch force prediction algorithm was tested with five volunteers and the results were evaluated using two criteria: normalized root mean squared error (NRMSE) and correlation (CORR). The training time for the subjects was only 2 min 29 sec, but the prediction results were successful with NRMSE = 0.093 ±0.047 and CORR = 0.957 ±0.031. These results imply that the proposed algorithm is useful to measure the generated pinch force without force sensors. The possible applications of the proposed method include controlling bionic finger robot systems to overcome finger paralysis or amputation.**

I. Introduction

THE dexterous manipulation skills of the human hand are encoded and controlled by the nervous system, which enables the production of voluntary motor actions. When humans lift and hold objects, the isometric grip (pinch) force, produced by the thumb and index finger tips, plays a decisive role in exerting a vertical force to oppose the object's weight [1]. The amount of force is adjusted appropriately by tactile sensations based on the object's different shapes, weights, and textures; excessive force may result in damage to the object, while too little force may result in dropping the object. The force that is exerted on the object increases or decreases according to the muscle activities, and these activities can be monitored using a surface electromyogram (sEMG).

sEMG, the recording of electric muscle activities on the skin surface, is a method of detecting the movement intentions of the user for human-robot interactions (HRI) such as robotic prostheses [2, 3] and teleoperation [4, 5]. These recordings are used widely because the signal is noninvasively detected and it precedes the actual body movements [6], thus it is faster than kinematic and dynamic devices such as force sensors and motion trackers. Tenore *et al.* and Nagata *et al.* have demonstrated the possibilities of individually distinguishing the flexion and extension of fingers using sEMG and have suggested the potential of controlling the individual fingers of a hand robot [7, 8]. They, however, only distinguished two states of movement, "ON" or "OFF", and did not try to extract information regarding force from the sEMG. When a subject pours water into a glass held by a robot hand controlled by sEMG, the glass could be dropped; this result from the force produced by robot to hold the object does not change as the weight of the held object increases.

There have been recent studies that predict muscle force, but most focused on wrist or elbow sections [9-11], not on hand sections. Challenging issues exist to match sEMG with finger force; first, too many (thirty-nine) muscles contribute the force and extraction of the individual muscle activities using surface electrodes is difficult because either most extrinsic muscles are located deep inside the hand or most intrinsic muscles are too small to observe [12]. Second, the signals on the skin surface are mixtures of signals generated by many active muscles resulting from crosstalk [13]. Third, the central nervous system combines muscles into groups and a desired grip force is generated by an infinite number of muscular activation patterns; furthermore, the relation

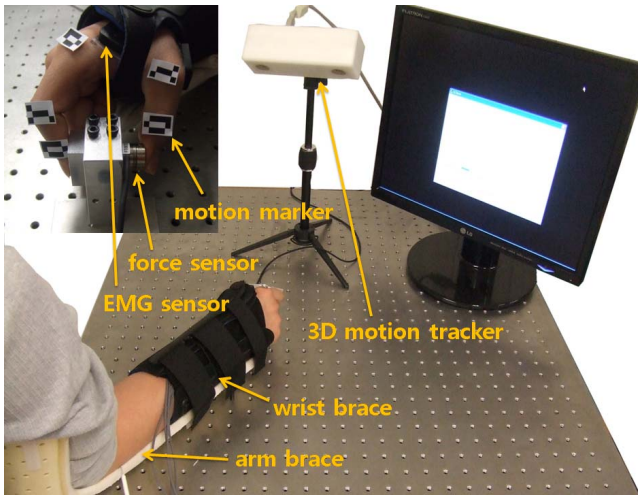

Fig. 1. Experimental setup.

Manuscript received April 10, 2008. This work was supported by the Korea Science and Engineering Foundation (KOSEF) grant funded by the Korean government (MOST) (No. R01-2007-000-11659-0).

C. Choi, S. Kwon, and M. Shin are with the Department of Mechanical Engineering, KAIST, Daejeon, Republic of Korea (e-mail: axlguitar; norierup; mihye@kaist.ac.kr).

W. Park is with the Robotics Program, KAIST, Daejeon, Republic of Korea (e-mail: park9039@kaist.ac.kr).

J. Kim is with the Department of Mechanical Engineering, KAIST, Daejeon, Republic of Korea (corresponding author; Tel.: +82-42-869-3231; Fax: +82-42-869-3210; e-mail: jungkim@kaist.ac.kr).

between the patterns and the force has not been clearly investigated [14]. Although there have been many studies that concurrently measure both finger forces and sEMG for motor rehabilitation or hand-related kinesiology studies [15, 16], the analyses were off-line and invasive electrodes were used. For finger force prediction from sEMG in HRI applications, the prediction model should be processed in real-time, and it involves two issues: 1) each subject's different muscle characteristics can be reflected in the force prediction in a short time, and 2) the model needs to be computationally fast.

To address these issues, an artificial neural network (ANN) may be an appropriate model and has been implemented in many real-time applications due to its ability to approximate complex nonlinear mappings directly from input values [17, 18]. The ANN, inspired by biological neural networks, is composed of a number of highly interconnected artificial neurons activated by external stimuli and provides a model for a large class of natural and artificial phenomena that are difficult to manage using classical parametric techniques. The primary advantage of using an ANN is that it acts as a black box model, so it does not require detailed information, such as the relation between sEMG and muscle force or biological phenomena, of the human muscular-skeleton system.

This paper presents a real-time isometric pinch force prediction algorithm for the measurement of the generated pinch force without using force sensors, which are expensive and require a bulky frame. To record muscle activities, seven surface electrodes were attached to the skin near to the muscles located in the hand or forearm, which make the thumb and index finger joint movements and are also observable using surface electrodes. Among these muscles, the most effective activities to extract the pinch force information were determined based on the Fisher linear discriminant paradigm, and the number of electrodes was reduced to four. The signals from the four sEMG electrodes were fed into the ANN with an optimized structure to predict the force.

II. Methods

A. Experimental Setup

The experimental setup is illustrated in Fig. 1. The subjects were requested to sit comfortably on a chair with their forearm flexed (90°) via an arm brace, which was fixed to an optical table, and with their wrist fixed using a wrist brace. The subject grasped a force sensor and an aluminum post with the thumb and index finger tips set 45 mm apart in opposition. A Nano 17 force sensor (ATI Industrial Automation, USA) was used to measure the force produced by the fingers; the sensor has a force resolution of 12.5 mN. The sensor was mounted on an aluminum post and covered with a cotton pad to prevent direct contact with the subject's skin, which could affect the temperature changes of the sensor and increase the electrical noise in the sEMG measurement. The activities of muscles were recorded and amplified 1000 times using bipolar noninvasive surface electrodes (DE-2.1, Delsys, USA) with built-in amplifiers. The electrodes were connected to the data acquisition board (PCI 6034e, National Instruments™, USA), which transmitted the signals to a computer at 1000 Hz. To verify that the experiment was performed under isometric conditions, an optical motion tracking system, Micron Tracker S60 (Claron Technology Inc., Canada), was used. Two markers were placed on the thumb at the distal and proximal interphalangeal joints and three markers were placed on the index finger at the metacarpophalangeal joint and the distal and proximal interphalangeal joints. On a monitor in front of the subject, three force levels were displayed as simple bars that represented the i) predrawn target force levels, ii) measured force levels, and iii) predicted force levels.

B. Signal Processing

It is well known that an EMG can be modeled as a zero mean Gaussian process [19]. Thus, the following equation was used to estimate the signal variance for feature extraction and the low-pass filter:

$$\hat{\sigma}^2 = \frac{\sum_{i=1}^{N} \left(M_i - \overline{M}\right)^2}{N-1}, \tag{1}$$

where M_i, N, and $\overline{M}$ are the magnitude of the i^{th} data, the length of the analysis window, and the mean of the magnitude of N, respectively. The function of variance is analogous to a moving average (MA) filter excluding the square term and denominator.

Like a moving average filter, the cut-off frequency, f_c, of the low-pass filter was defined in relation to the moving average filter as follows.

$$f_c = \frac{f_s}{2N}, \tag{2}$$

where f_s and N are the sampling frequency and analysis window length, respectively. This equation describes that the effectiveness of the low-pass filter increases with a larger window because the cutoff frequency decreases; thus, high frequency noises are effectively reduced. In contrast, the large window introduces a significant time delay and this delay can become an obstacle for a natural real-time HRI. Hence, there is a tradeoff between the real-time signal process and the accuracy of the pattern recognition. Considering these aspects of the measurement, the length of the analysis window was empirically determined to be 200 ms.

C. Myoelectricsite selection

There are 15 muscles that control the thumb and index finger, but only half of their activities are observable via sEMG. A software package, ADAM Interactive Anatomy (A.D.A.M. Inc., USA), was used to find which of these muscles are located in the outermost layer among the muscles in the forearm and the hand. From the software, it was assumed that seven muscle activities could be observed:

Fig. 2. Seven electrode placements for the sEMG signal extraction. The images of wires were removed for clear expression of the placement.

Extensor Digitorium (ED), Abductor Pollicis Longus (APL), Flexor Digitorum Superficialis (FDS), Dorsal Interosseous (DI), Abductor Pollicis Brevis (APB), Flexor Pollicis Brevis (FPB), and Adductor Pollicis (AP).

To obtain the seven target muscles' activities, seven electrodes were attached to a volunteer's forearm and hand, and channels 1 to 7 were targeted to obtain the activities of the ED, APL, FDS DI, APB, FPB, and AP muscles, respectively as shown in Fig. 2. The pinch task with static and dynamic force guidance was performed five times while recording the sEMG and force data as shown in Fig. 3. However, the activity of the FPB could not be observed because the electrode was too wide to detect its activities, most parts of which were covered by the APB; the channel 6 signal was recorded from the APB, which lies primarily in the outer layer of the palm. Even though the signals in channels 5 and 6 were recorded from the same muscle, each signal represents different activities. This is because each whole muscle is innervated by a number of motor units and the units' functional characteristics differ depending on the specific functions, such as the contraction velocity and twitch force [20].

It was expected that all signals would not be helpful in extracting the force information; for instance, Fig. 3 shows

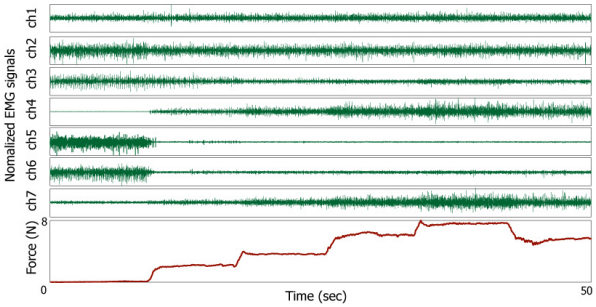

Fig. 3. The activities of the seven muscles during the pinch force generation.

that the signal from channel 1 seems to be independent on the measured force over time. To determine which channel is relatively effective in extracting the force information, the Fisher linear discriminant paradigm was employed [21]. This paradigm has been used widely in face recognition research [22, 23] and provides the criterion function:

$$J_k = \frac{\left|\hat{m}_1 - \hat{m}_2\right|^2}{\hat{s}_1^{\,2} + \hat{s}_2^{\,2}}. \tag{3}$$

This function is for a two-class pattern recognition problem; the subscript k on the left-hand side and subscripts 1 and 2 on the right-hand side indicate the sEMG channel and classes 1 and 2, respectively. $\hat{m}_i$ indicates the sample mean of the ith class, and $\hat{s}_i^{\,2}$ indicates the sample variance of the ith class as follows:

$$\hat{m}_i = \frac{1}{N}\sum_{\mathbf{x}\in D_i}\mathbf{x}, \tag{4}$$

$$\hat{s}_i^{\,2} = \frac{1}{N-1}\sum_{\mathbf{x}\in D_i}\left(\mathbf{x} - \hat{m}_i\right)^2. \tag{5}$$

N is the number of samples and x is a vector of the filtered signals. The numerator represents the difference of the sample means of the two-classes, and the higher the difference, the easier the samples can be separated. The denominator represents the amount of variance in the samples of both classes, and the smaller the variance, the better the samples can be identified into each class. Therefore, when Jk is high, the signals at the kth channel provide effective information for successful classification.

Our research goal was not to classify the two classes of sEMG, but to choose more discriminable channels: class 1 of the signals when the force was low (0 N) and class 2 of the

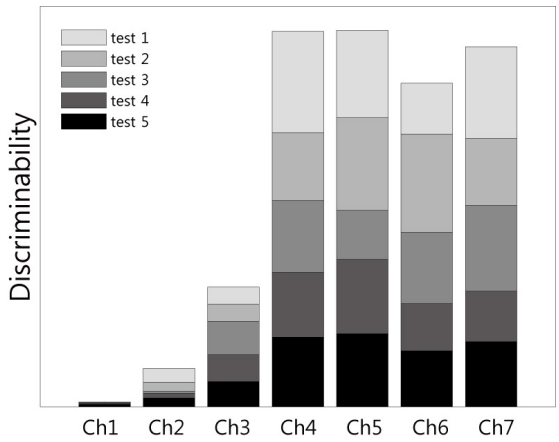

Fig. 4. Discriminabilities (J_k) of the signals measured by the seven channel electrodes based on the Fisher linear discriminant paradigm. These discriminabilites were evaluated using five test data, and each discriminability was cumulated according to the channel. A high J_k indicates that the signals at the k^{th} channel provide useful information for successfully predicting the pinch force.

signals when the force was high (8 N). Because the sEMG has a proportional relation to muscle force, if the signals at a certain channel provide the most discriminable information between the high and low forces, they could also represent a middle range of force better than the signals in the other channels. Using five test data sets, the discriminabilities were evaluated as shown in Fig. 4; it was concluded that the signals in channels 4 to 7 provided proper information to match the sEMG to the pinch force. Therefore, the signals from the channel 4 to 7 were only fed into ANN to predict the force.

D. Artificial Neural Network

As mentioned earlier, an ANN provides a black box model for a large class of natural and artificial phenomena that are difficult to manage using classical parametric techniques. In order to design the network, a set of signals flow through the network; then, the network adjusts its internal structure until it reaches a stable state in which the outputs are considered satisfactory. After successful training, the network is preserved, receives unseen input values, and processes the data to produce appropriate outputs. The performance depends on various factors, the most important of which is to determine the network structure with the degree of freedom or information that is inherent in the training data. The structure may contain several hidden layers, however one hidden layer is sufficient to guarantee convergence in the training according to the Universal Approximation Theorem [24]. In contrast to the number of hidden layers, the theorem does not specify the number of hidden neurons, so it must be determined by trial and error. The number should be considered according to the degree of nonlinearities between the input and output samples; however, it is difficult to define the nonlinearities between the sEMG and the muscle forces.

A choice of the optimal number of neurons is important and results in significant effects on the network performance. From a computational viewpoint, the network demands the fewest hidden neurons to reduce the number of interconnections, whose weights should be updated during training. Furthermore, an excessive number of hidden neurons can generate over-fitting problems in which the network loses its generalization abilities. Conversely, a network with too few neurons, with respect to the complexity of the problem, might not be able to effectively learn the training data. Therefore, the use of an optimal number of hidden neurons is highly desirable for efficient training.

To determine the optimal number of hidden neurons, an off-line ANN simulation was performed using five test data sets; one set was used for training and the other sets were used for testing. ANN performances with many neurons (1 – 40) were evaluated, and the tests were performed with each number of neurons 10 times. The performance was evaluated using two criteria: normalized root mean squared error (NRMSE) and correlation (CORR).

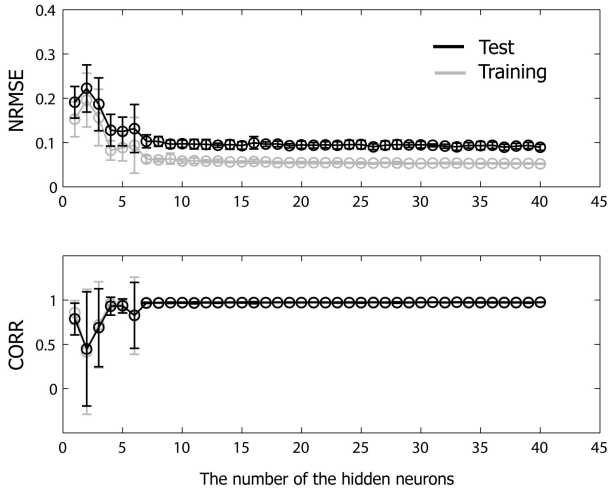

Fig. 5. ANN simulation results for determining the optimal number of hidden neurons in a hidden layer. The prediction accuracies were evaluated using two criteria: normalized root mean squared error (NRMSE) and correlation (CORR).

$$\mathrm{NRMSE} = \frac{\sqrt{\sum \left(\mathbf{x}_{1,i} - \mathbf{x}_{2,i}\right)^2}}{\mathbf{x}_{\max} - \mathbf{x}_{\min}} \tag{6}$$

$$\mathrm{CORR} = \frac{N\sum \mathbf{x}_{1,i}\mathbf{x}_{2,i} - \sum \mathbf{x}_{1,i}\sum \mathbf{x}_{2,i}}{\sqrt{N\sum \mathbf{x}_{1,i}{}^2 - \left(\sum \mathbf{x}_{1,i}\right)^2}\sqrt{N\sum \mathbf{x}_{2,i}{}^2 - \left(\sum \mathbf{x}_{2,i}\right)^2}} \tag{7}$$

x1, x2, and N indicate the force measured by the sensor, the predicted force from the ANN, and the total number of data, respectively; subscript i indicates the i^{th} data. Figure 5 suggests that ten hidden neurons are sufficient to satisfy the tradeoff between computational efficiency and sufficient training.

During the training stage, all subjects were instructed to produce pinch forces following the bars displayed in static and dynamic levels: the force and sEMG were recorded concurrently. Next, the sEMGs were filtered and the network was trained using the filtered samples. Network tuning was performed using a backpropagation algorithm (learning rate = 0.8) with a momentum approach (momentum rate = 0.3) [24].

E. Tasks and Procedures

Five male subjects, aged 26.4 years (SD 2.3), volunteered in the experiments. All participants reported no history of upper extremity or other musculoskeletal complaints. The subjects were required to exert pinch forces with their right hand under the isometric conditions. They were asked to fully relax their forearm muscles, to avoid exerting any other forces except the pinch force, and to hold the pinch pose. Prior to the experiments, all subjects were instructed on how to produce the pinch force, and the positions of the corresponding muscles (which were selected in the myoelectricsite selection) were detected through palpation. The best sites for clear detection of the muscle contractions were then found while slightly moving the electrode. Next, the four electrodes were attached to the best site on the skin using adhesive tape.

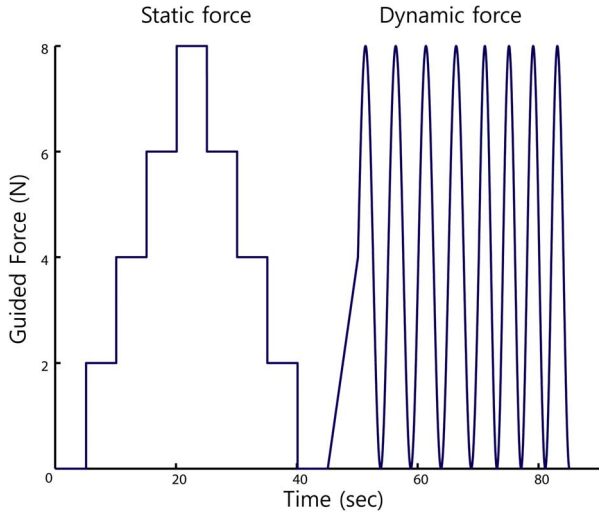

Fig. 6. The guided force levels with static and dynamic functions for the ANN training.

The experiments consisted of two parts: a training part to train the ANN and a test part for verification. Each part was performed with ten trials. In the training part, the subjects were requested to exert the target force levels, which were displayed on the monitor, for 85 seconds. The levels were composed of static (2, 4, 6, 8 N) and dynamic levels by generating a sinusoidal function as shown in Fig. 6. In the test part, there are two sessions: the first session verified whether the ANN training was successfully completed and the second session checked whether the ANN had generalization properties using unpredicted input. In the first session, the subjects were instructed to exert force using the same protocols as the training part with the force guidance, in which the predicted force was not displayed to prevent the estimated force adapting to the measured force. In the second session, the subjects were asked to produce voluntarily forces for 60 seconds.

III. Experimental Results and Discussion

The sEMG from the four electrodes were used as inputs in the optimized ANN, and the forces from the force sensor were used as references. Figure 7 shows one of the experimental results of both session 1 and session 2; the gray line indicates the measured force from the sensor and the black line indicates the force predicted by the ANN. To validate the prediction method, the predicted data were evaluated against the measured data using two criteria: NRMSE and CORR. In session 1, as mentioned earlier, the subjects were required to exert target force levels for 85 seconds. Since these profiles had the same tendency as the profiles during the ANN training, the good performance (NRMSE = 0.093 ±0.047 and CORR = 0.957 ±0.031) for all subjects was validated. In session 2, the subjects could produce any force, so the forces had a tendency that the ANN could not expect. It is interesting that the results of session 2 (NRMSE = 0.112 ±0.082 and CORR = 0.932 ±0.058) were comparable with those of session 1 as a result of the ANN's generalization abilities.

TABLE I
Experimental Results on the Force Prediction with Five Subjects

Subjects	Session 1		Session 2	
	NRMSE	CORR	NRMSE	CORR
S1	0.110 ±0.026	0.946 ±0.024	0.130 ±0.064	0.924 ±0.042
S2	0.085 ±0.019	0.962 ±0.011	0.102 ±0.024	0.940 ±0.014
S3	0.108 ±0.027	0.942 ±0.015	0.124 ±0.030	0.915 ±0.014
S4	0.077 ±0.011	0.967 ±0.006	0.104 ±0.019	0.935 ±0.029
S5	0.085 ±0.018	0.966 ±0.007	0.101 ±0.027	0.945 ±0.018
Average	0.093 ±0.047	0.957 ±0.031	0.112 ±0.082	0.932 ±0.058

Prior the experiments, the sEMG samples were collected to train the ANN, where approximately 85 seconds were required, and then the training was performed with a limited number of iterations (= 100), where approximately only 64 seconds were required in a computer running on a Pentium 4, 2.93 GHz processor. The total time for the sample collection and ANN training was fast (2 min 29 sec). It was believed that the reduction of the number of inputs (electrodes) reduced the training time because the excluded channels provided less productive information in predicting the force. Without the exclusions, the number of weights in the network would have increased as the number of input neurons increased; also, it is difficult to tune the weights using less productive information. It is well known that individuals have anatomical variations in their muscles [12] and the sEMG depends significantly on the individual skin and muscle properties. In addition, the positioning the electrodes differently would produce different recordings, even for observations of the same muscle [26]. Therefore, a user specific ANN model is required, and also whenever a user wants to use the force prediction model from

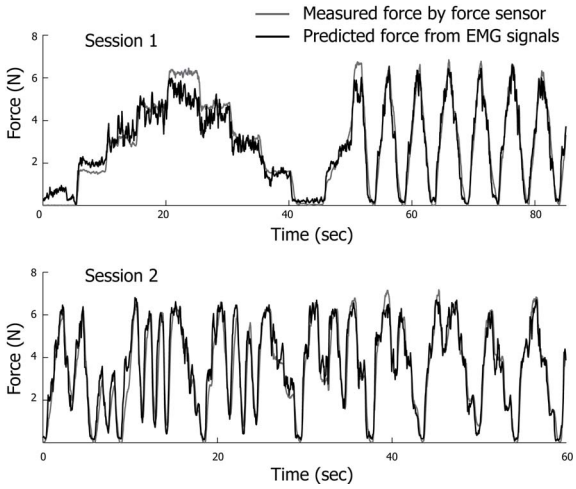

Fig. 7. The prediction results using the ANN. The gray line indicates the measured force from the sensor and the black line indicates the force predicted by the ANN. Session 1 was performed with the target force levels, which were displayed on the monitor. But in session 2, the subjects could produce any force they want.

sEMG, the training step is necessary prior to use. The short training time implies that this model is practical and the user is able to use it without time consuming work.

These experiments were performed by measuring the pinch forces produced by the thumb and index finger tips that were set 45 mm apart in opposition, and the experimental result shows that the pinch forces were well predictable from the sEMG. However, if two fingers, more or less than 45 mm apart in opposition, produce the forces, the designed model is not guaranteed to provide accurate predictions. The muscle forces are dependent on the muscle lengths [20], and if the distance of the two fingers changes, the brain would control the muscles in a different way.

IV. Conclusions

The main objective of this paper is to present an algorithm for real-time pinch force prediction and the evaluation results of the five volunteer subjects. Considering the experimental results, the designed ANN with an optimized structure successfully predicted the pinch force from four sEMG electrodes. In addition, the training time was short, which implies that the proposed method is practical for the measurement of the generated pinch force without force sensors. A possible application of the pinch force prediction method could be in controlling several platforms, such as bionic finger robot systems for finger paralysis or amputation (i.e. involving exoskeletons and finger prostheses), and teleoperated robotic systems that can perform human tasks in hazardous environments.

The above discussion has important implications for future work on improving the pinch force prediction from sEMG with regards to the distances between the thumb and index finger tips. For this purpose, we are developing a motorized pinch force measurement device and will undertake an extended study under dynamic kinematic conditions. Another possible extension of this study is the prediction of five finger forces using sEMG with the aim of controlling fingers of a robotic hand with the appropriate forces.

References

[1] G. Westling and R. S. Johansson, "Factors influencing the force control during precision grip," *Exp Brain Res*, vol. 53, pp. 277-84, 1984.

[2] B. Dellon and Y. Matsuoka, "Prosthetics, exoskeletons, and rehabilitation - Now and for the future," *IEEE Robotics & Automation Magazine*, vol. 14, pp. 30-34, 2007.

[3] C. Cipriani, F. Zaccone, S. Micera, and M. C. Carrozza, "On the shared control of an EMG-controlled prosthetic hand: Analysis of user-prosthesis interaction," *IEEE Trans Robot*, vol. 24, pp. 170-184, 2008.

[4] P. K. Artemiadis and K. J. Kyriakopoulos, "EMG-based teleoperation of a robot arm in planar catching movements using ARMAX model and trajectory monitoring techniques," in *Proc. 2006 IEEE Int. Conf. Robotics and Automation*, 2006, pp. 3244-3249.

[5] O. Fukuda, T. Tsuji, M. Kaneko, and A. Otsuka, "A human-assisting manipulator teleoperated by EMG signals and arm motions," *IEEE Trans Robot Automat*, vol. 19, pp. 210-222, 2003.

[6] P. R. Cavanagh and P. V. Komi, "Electromechanical delay in human skeletal muscle under concentric and eccentric contractions," *Eur J Appl Physiol Occup Physiol*, vol. 42, pp. 159-63, 1979.

[7] F. Tenore, A. Ramos, A. Fahmy, S. Acharya, R. Etienne-Cummings, and N. V. Thakor, "Towards the Control of Individual Fingers of a Prosthetic Hand Using Surface EMG Signals," in *29th Annu. Int. Conf. IEEE Engineering in Medicine and Biology Society*, A. Ramos, Ed., 2007, pp. 6145-6148.

[8] K. Nagata, K. Ando, K. Magatani, and M. Yamada, "Development of the hand motion recognition system based on surface EMG using suitable measurement channels for pattern recognition," in *29th Annu. Int. Conf. IEEE Engineering in Medicine and Biology Society*, K. Ando, Ed., 2007, pp. 5214-5217.

[9] E. E. Cavallaro, J. Rosen, J. C. Perry, and S. Burns, "Real-time myoprocessors for a neural controlled powered exoskeleton arm," *IEEE Trans Biomed Eng*, vol. 53, pp. 2387-96, 2006.

[10] F. Mobasser, J. M. Eklund, and K. Hashtrudi-Zaad, "Estimation of elbow-induced wrist force with EMG signals using fast orthogonal search," *IEEE Trans Biomed Eng*, vol. 54, pp. 683-93, 2007.

[11] D. Staudenmann, I. Kingma, A. Daffertshofer, D. F. Stegeman, and J. H. van Dieen, "Improving EMG-based muscle force estimation by using a high-density EMG grid and principal component analysis," *IEEE Trans Biomed Eng*, vol. 53, pp. 712-9, 2006.

[12] [H.-L. Yu, R. A. Chase, and B. Strauch, Atlas of hand anatomy and clinical implications. St. Louis: Mosby, 2004.

[13] C. J. De Luca and R. Merletti, "Surface myoelectric signal cross-talk among muscles of the leg," *Electroencephalogr Clin Neurophysiol*, vol. 69, pp. 568-75, 1988.

[14] M. A. Maier and M. C. Hepp-Reymond, "EMG activation patterns during force production in precision grip. II. Muscular synergies in the spatial and temporal domain," *Exp Brain Res*, vol. 103, pp. 123-36, 1995.

[15] F. J. Valero-Cuevas, F. E. Zajac, and C. G. Burgar, "Large index-fingertip forces are produced by subject-independent patterns of muscle excitation," *J Biomech*, vol. 31, pp. 693-703, 1998.

[16] M. A. Maier and M. C. Hepp-Reymond, "EMG activation patterns during force production in precision grip. I. Contribution of 15 finger muscles to isometric force," *Exp Brain Res*, vol. 103, pp. 108-22, 1995.

[17] S. X. Yang and M. Q. H. Meng, "Real-time collision-free motion planning of a mobile robot using a neural dynamics-based approach," *IEEE Trans Neural Networks*, vol. 14, pp. 1541-1552, 2003.

[18] J. U. Chu, I. Moon, Y. J. Lee, S. K. Kim, and M. S. Mun, "A supervised feature-projection-based real-time EMG pattern recognition for multifunction myoelectric hand control," *IEEE Trans Mechatron*, vol. 12, pp. 282-290, 2007.

[19] E. Shwedyk, R. Balasubramanian, and R. N. Scott, "Nonstationary Model for Electromyogram," *IEEE Trans Biomed Eng*, vol. 24, pp. 417-424, 1977.

[20] A. Freivalds, Biomechanics of the Upper Limbs: Mechanics, Modelling and Musculoskeletal Injuries. Boca Raton, FL: CRC Press, 2004.

[21] R. O. Duda, P. E. Hart, and D. G. Stork, Pattern classification, 2nd ed. New York: Wiley, 2001.

[22] L. F. Chen, H. Y. M. Liao, M. T. Ko, J. C. Lin, and G. J. Yu, "A new LDA-based face recognition system which can solve the small sample size problem," *Pattern Recognition*, vol. 33, pp. 1713-1726, 2000.

[23] H. Yu and H. Yang, "A direct LDA algorithm for high-dimensional data - with application to face recognition," *Pattern Recognition*, vol. 34, pp. 2067-2070, 2001.

[24] S. S. Haykin, Neural networks: a comprehensive foundation. New York: Maxwell Macmillan International, 1994.